

Graphene for Reconfigurable Terahertz Optoelectronics

This paper addresses the potential to design reconfigurable terahertz devices using electrically tunable optical properties in modulators and switches that are based on graphene.

By BERARDI SENSALÉ-RODRÍGUEZ, *Student Member IEEE*, RUSEN YAN, LEI LIU, *Member IEEE*, DEBDEEP JENA, *Member IEEE*, AND HUILI GRACE XING, *Member IEEE*

ABSTRACT | In this paper, we examine graphene as a material for reconfigurable terahertz (THz) optoelectronics. The ability of electrically tuning its optical properties in a wide range of THz frequencies, together with its 2-D nature and facile integration, leads to unique opportunities for inventing novel THz devices as well as for extending the performance of existing THz technologies. We first review progress in graphene THz active optoelectronic components to date, including large-area graphene, plasmonic, and metamaterial-based devices. Advanced designs and associated challenges are then discussed.

KEYWORDS | Active tuning; filters; graphene; metamaterials; modulators; plasmonics; reconfigurable; switches; terahertz (THz)

I. INTRODUCTION

Promising applications in many diverse areas of human endeavor, including medicine, biology, communications, security, astronomy, etc., terahertz (THz) technology has recently turned into an active area of scientific research [1]–[3]. The THz frequency band, usually defined in the 0.1–30-THz range, was for decades one of the least explored regions of the electromagnetic spectrum, mainly due to the lack of materials and devices responding to these frequencies in a controllable manner. However, THz technology has lately gained increased attention for industrial and commercial applications as the performance of THz

emitters and detectors improve. For instance, THz imaging is appealing for several medical and security applications (e.g., dentistry imaging [5], *in vivo* skin cancer detection [6], personal scanners [7], etc.), since THz waves enable higher spatial resolution than longer wavelength radiations (e.g., millimeter waves) and are nonionizing [8] in contrast to shorter wavelength waves (e.g., ultraviolet and X-rays). There is important spectroscopic information lying in the THz frequency range, which makes THz spectroscopy a useful technique for thin film characterization [9], biological applications [10], and detection of illegal substances (i.e., explosives, drugs, etc.) [11]. Furthermore, since THz waves allow for larger bandwidth than radio frequency (RF) and microwaves, and are less susceptible to scintillation effects than infrared (IR) radiation [12], certain frequency bands lying in the THz range have been proposed for short-range wireless communications [13]–[15].

The recent progress in THz sources and detectors, as well as the blooming of application proposals, fostered the necessity to develop devices capable of actively manipulating THz waves including: switches, modulators, filters, polarizers, etc., which can be broadly termed as reconfigurable THz optoelectronic components. Reconfigurable components can reduce the complexity, cost, and dimensions of THz systems. To this end, various approaches have been investigated over the past decade to tune the effective THz permittivity, including electrical, optical, plasmonic, mechanical, thermal, structural (i.e., phase change materials) means, etc. [16]–[20]. Both the real and imaginary parts of the permittivity can be potentially tuned. In this paper, we limit our discussions primarily to tuning of the imaginary part of the permittivity. Among all the driving mechanisms, electrical tuning is the most attractive, considering its integrability and reliability.

Electrical tuning of the imaginary part of the permittivity is typically implemented with semiconductors by

Manuscript received June 15, 2012; revised January 15, 2013; accepted February 23, 2013. Date of publication March 27, 2013; date of current version June 14, 2013.

This work was supported by the National Science Foundation (NSF) CAREER ECCS-084910 (Anupamu Kaul), ECCS-1002088 (George Haddad), ECCS-1202452 (Samir El-Ghazaly), AFOSR FA9550-12-1-0257 (James Hwang), the Center for Advanced Diagnostics and Therapeutics (AD&T), and the Center for Nanoscience and Technology (NDnano), University of Notre Dame, Notre Dame, IN, USA.

The authors are with the Department of Electrical Engineering, University of Notre Dame, Notre Dame, IN 46556 USA (e-mail: bsensale@nd.edu; hxing@nd.edu).

Digital Object Identifier: 10.1109/JPROC.2013.2250471

tuning their electrical conductivity. Though, to date, a handful of groups have demonstrated proof-of-concept results, nearly all the resultant devices showed high insertion loss (IL) and compromised reconfigurability. In this context, graphene has emerged as a highly promising material because of its capability to efficiently manipulate THz radiation meanwhile introducing negligible insertion loss [21], [22]. Furthermore, since graphene is structurally flexible, easily transferable, and inexpensive to produce, it offers unprecedented freedom to construct reconfigurable THz devices or system-on-a-chip solutions. Despite the immaturity and short history of graphene as a THz material, the measured and predicted performance of graphene-based devices is already among the best reported to date. This is remarkable, especially considering that graphene is atomically thin. In this paper, we provide an overview of the underlying principles of graphene-based reconfigurable THz components, the state of the art, several novel device proposals as well as the challenges we currently face.

II. OPTICAL PROPERTIES OF GRAPHENE IN THE THz/IR RANGE

Although many proposed applications of graphene, a one-atom-thick layer of sp^2 -bonded carbon with a honeycomb lattice, rely on its electronic properties [23], [24], its optical properties, inherited also from its singular conical band structure [Fig. 1(a)], are equally noteworthy [25].

A. Intraband and Interband Transitions in Graphene

The imaginary part of the permittivity of a material is associated with loss or absorption of electromagnetic waves, which is in turn proportional to the real part of its optical conductivity. To understand the tunability of optical absorption in graphene, we need to first take a look at what determines its optical conductivity. Optical transitions (thus absorption) in graphene include intraband and interband transitions, as depicted in Fig. 1(a). Based on linearization of the tight binding Hamiltonian of graphene near the $K(K')$ points (i.e., the Dirac points) of the first Brillouin zone, its optical conductivity can be expressed as the sum of the two contributions [26]–[28]

$$\sigma(\omega) = \sigma_{\text{intra}}(\omega) + \sigma_{\text{inter}}(\omega) \quad (1)$$

where

$$\begin{aligned} \sigma_{\text{intra}}(\omega) &= \frac{ie^2 E_f}{\pi \hbar^2 (\omega + i/\tau)} \\ \sigma_{\text{inter}}(\omega) &= \frac{ie^2 \omega}{\pi} \int_0^\infty \frac{f(\varepsilon - E_f) - f(-\varepsilon - E_f)}{(2\varepsilon)^2 - (\hbar\omega + i\Gamma)^2} d\varepsilon. \end{aligned} \quad (2)$$

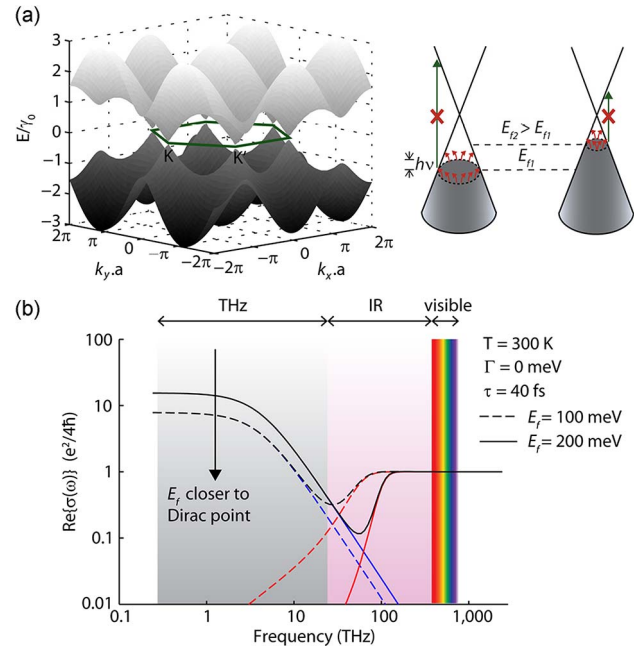


Fig. 1. (a) Band structure of graphene and sketch of the possible optical transitions: interband (green) and intraband (red); in the THz range intraband transitions are dominant and optical conductivity depends on the density of states available for intraband transitions, thus Fermi level. (b) Real part of the optical conductivity in graphene versus frequency [according to (1) and (2)]. The contribution from intraband transitions is plotted in blue, while the contribution from interband transitions is plotted in red. The dependence of optical conductivity with Fermi level, thus tunability, is high in the THz/IR region and reduces to zero for the visible range or higher frequencies.

Here, e is the electron charge, \hbar is the reduced Planck constant, ω is angular frequency, E_f is the Fermi level, $f(\cdot)$ is the Fermi distribution function, τ is momentum relaxation time, and Γ is a parameter describing the broadening of interband transitions. In (2), it is assumed that $E_f \gg k_B T$.

At low frequencies, thus low photon energies, the graphene optical conductivity is mainly determined by intraband transitions, while at high frequencies, the contribution of interband transitions becomes dominant, as shown in Fig. 1(b). By taking the limit $\omega \rightarrow \infty$ in [(1) and (2)] it follows that, at very high frequencies including the visible range, its optical conductivity reduces to a constant value of $e^2/4\hbar$, thus a universal absorption per graphene layer of $\sim 2.3\%$ at normal incidence [29]. Based on this property, graphene has been actively pursued as a material for transparent-flexible electrodes [30].

The dependence of optical conductivity with Fermi level indicates that the graphene optical conductivity can be modified by controlling the Fermi level, i.e., carrier concentration. In the IR range, this leads to a finite absorption modulation of from $\sim 0\%$ to 2.3% at normal incidence [31], [32]. Though this absorption modulation is

weak, several tunable devices such as mode-lock lasers [33] and ultrafast electroabsorption IR modulators [34]–[36] have been experimentally demonstrated employing graphene based on tuning of its interband transitions. Enhanced modulation has also been theoretically proposed by taking advantage of plasmonic resonances in graphene [37]. Theoretical evaluation [36] shows that there are several competitive advantages when comparing graphene to conventional semiconductor-based IR modulators. On the other hand, in the THz range, the contribution from interband transitions to the optical conductivity becomes negligible. As a result, the real part of the graphene conductivity can be written in a Drude-like dispersion form

$$\sigma(\omega) = \sigma_{dc}/(1 + \omega^2\tau^2) \quad (3)$$

where σ_{dc} is the direct current (dc) electrical conductivity. In a 2-D semiconductor with classical parabolic energy dispersion, the dc conductivity is linearly proportional to the carrier concentration, $\sigma_{dc} \propto E_f \propto n$, to the first order of approximation [38]. In graphene, the dependence is nonlinear owing to its conical dispersion: $\sigma_{dc} \propto E_f \propto \sqrt{n}$ [39], [40]. Therefore, for $\omega < \omega_0 = 1/\tau$ (ω_0 depends on graphene quality and is typically between 1 and 4 THz), the THz optical conductivity closely follows the electrical conductivity, which can be in turn effectively tuned [21], [22], [41], [42]. Depicted in Fig. 1(b) is the calculated real part of the conductivity for two Fermi levels at 300 K, assuming a momentum relaxation time of 40 fs, showing a clear change in the THz/IR range, while remaining constant for the visible. As frequency increases, the optical conductivity, thus THz absorption, by large-area graphene typically rolls off. However, by employing patterned structures that enable plasmonic resonances [43], [44], the effective optical conductivity can still be greatly enhanced, which will be discussed below.

B. Plasmons in Graphene

Plasmons are collective oscillations of charge carriers [45], [46], which can occur in both bulk graphene (i.e., large area) or patterned graphene, in analogy to the so-called propagating and localized plasmons in planar and patterned metals or traditional semiconductor 2-D electron gases (2DEGs), respectively [47]. Early theoretical studies of plasmons in graphene [48]–[53], with several posterior experimental demonstrations [54], [55], were mainly oriented toward large-area graphene at IR frequencies, i.e., unconfined propagating plasmons. In the THz frequency range, Ryzhii *et al.* calculated properties of gated THz plasmons in graphene, providing a basis for designing reconfigurable plasmonic devices [56], [57]; Rana *et al.* proposed THz lasing based on plasmons in graphene [58]. Yet, study of plasmons in patterned structures allows for a simpler understanding of its characteristics and how they

are related with the electrical properties of graphene [43], [44]. Furthermore, the plasmon propagation length in graphene [54], [55] is in the neighborhood of one micrometer, which is comparable to the THz plasmon wavelength. Consequently, propagating plasmons in graphene most likely play more important roles in IR than THz. To this end, we focus our discussions in this paper on localized plasmons.

The origin and properties of plasmons in patterned graphene at THz frequencies can be readily derived starting from the Drude optical conductivity. Arrays of patterned graphene with pattern dimensions smaller than the THz wavelength, including ribbons [43] and disks [44], as depicted in Fig. 2(a), can be understood as *R-L-C* resonators [59], [60]. The resistance *R* arises from the real part of resistivity [inverse of (3)] and is dependent on the geometry and dimension of the pattern. In the same fashion, the inductance *L*, usually referred in the literature as “kinetic inductance” [61], arises from the imaginary part of resistivity and is also inversely proportional to σ_{dc} . The capacitance *C* heavily depends on the pattern geometry and the interactions between adjacent elements of the array, which can be regarded as independent on the electrical properties of graphene. Therefore, the resultant plasmon resonance $\omega_p \propto 1/\sqrt{LC}$ is proportional to $\sqrt{\sigma_{dc}}$. Employing classical electromagnetic analysis based on the Maxwell–Garnett theory, a more rigorous derivation of these

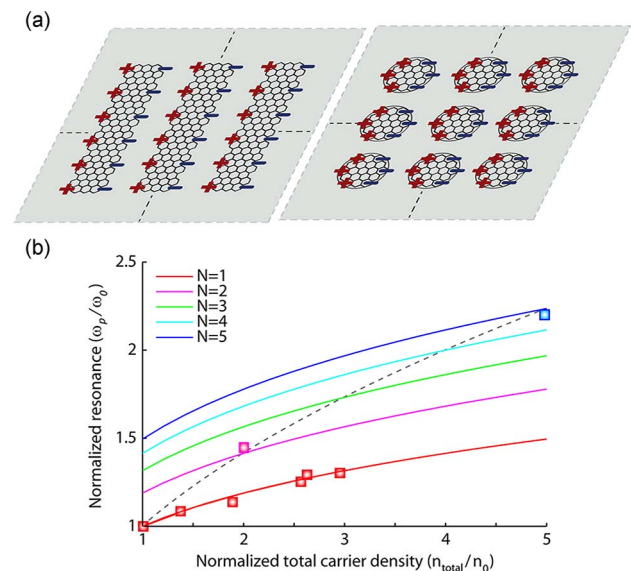


Fig. 2. (a) Sketch of graphene ribbon and disk subwavelength plasmonic structures highlighting charge distribution at the plasmon resonance frequencies. (b) Normalized plasmon resonance versus normalized total carrier density for an optically thin plasmonic structure composed of N number of graphene layers separated by insulators with each layer doped with n_0 carriers. Square markers represent experimental data extracted from [63]. The dash line is the square root of N , showing a good agreement with the experimental results.

dependences can be obtained [62], [63]. The dependence of ω_p on σ_{dc} in graphene is exactly the same with that in traditional semiconductors, and the plasmon resonance falls in the THz range for both materials. However, because of $\sigma_{dc} \propto E_f \propto \sqrt{n}$ in graphene, a signature of massless Dirac fermions, we obtain $\omega_p \propto \sqrt{\sigma_{dc}} \propto n^{1/4}$ in graphene instead of the square-root dependence in conventional semiconductors $\omega_p \propto \sqrt{\sigma_{dc}} \propto n^{1/2}$. This $n^{1/4}$ plasmon dispersion is identical to the case of gated graphene plasmons discussed in [56] and [57], thus ω_p has a $(V_g - V_{th})^{1/4}$ dependency where $V_g - V_{th}$ is the gate voltage swing or overdrive. With increasing carrier concentration, i.e., gate voltage swing in gated structures, the plasmon frequency increases.

Recently, Yan *et al.* reported another method to increase the plasmon resonance frequency by stacking several doped-graphene layers (doping concentration of n_0 for each layer) with polymer insulators of tens of nanometers of thickness in between [63]. To understand this result, we plot the dependence of plasmon frequency on the total charge density $n_{total} = Nn_0$, where N is the number of graphene layers, as shown in Fig. 2(b). Since the stacked structure is optically much thinner than the THz wavelength, its effective conductivity is $N\sigma_{dc,0}$, where $\sigma_{dc,0}$ is the conductivity of each layer. As a result, we obtain $\omega_p \propto N^{1/4}n_{total}^{1/4}$ or $\omega_p \propto N^{1/2}n_0^{1/4}$, which is consistent with the square-root dependence on N observed experimentally.

Interestingly, at plasmon resonance, when the inter-pattern capacitance is negligible, the effective THz optical conductivity of patterned graphene becomes independent of frequency: $\sigma_{eff} = f\sigma_{total,dc}$, where f is a filling factor accounting for the fraction of the area covered by graphene. Hence, plasmonic structures can extend the tunable range to THz frequencies higher than that limited by the carrier momentum scattering time.

In summary, comparable magnitude of absorption modulation in graphene structures can be achieved over a wide range of frequencies in the THz (Drude conductivity) and far-IR (plasmonic effects) region. The active control of THz optical conductivity by tuning the Fermi level is the driving mechanism in the reconfigurable devices discussed in this paper.

III. STATUS

Before looking with more depth into THz reconfigurable devices based on graphene, it is illuminating to briefly discuss the state of the art of the electrically reconfigurable THz devices in order to understand the limitations and challenges of current technologies.

In terms of modulators and switches, there have been a number of successful device implementations where the modulation mechanism is a voltage-induced change of the electrical, thus optical, conductivity. In this context, active terahertz metamaterial devices have been one of the most

promising alternatives for efficient THz modulation [4], [18], [64]–[66]. Therein, the change of conductivity, and, therefore, free carrier absorption in a small semiconductor active region located between a periodic metallic pattern, i.e., a frequency-selective surface structure (FSS), translates to an extraordinary control of the terahertz transmittance for frequencies close to the metamaterial intrinsic resonance. This active tuning can be understood on the basis of a change in capacitance or inductance of the FSS [17]. However, these devices are intrinsically narrowband. Devices based on large area semiconductor heterostructures can provide intrinsically broadband modulation, but the experimentally demonstrated modulation depths to date are very low ($\sim 6\%$ intensity modulation) [67], [68].

Several devices have also been proposed in which the dependence of the optical conductivity or refractive index with applied electric field is based on phenomena other than electrical conductivity tuning. For example, applying a static or low-frequency electric field in ferroelectric materials has been shown to modulate terahertz waves [69]. Several numerical studies show that microelectromechanical systems (MEMS) can potentially achieve close to 100% intensity modulation [19]. However, these devices need to be yet experimentally demonstrated. Additionally, filters with tunable characteristic frequency can operate as terahertz modulators. Active filters have been developed primarily for low frequencies, up to the millimeter wave (around 100 GHz) [70], while lately, tunable high-Q THz bandpass filters have been proposed [71] with a few preliminary experimental demonstrations [72]. One implementation is based on 3-D metallic photonic crystals sandwiching layers of liquid crystal: applied bias aligns the molecules thus tuning the refractive index. These devices might be used as modulators for their large modulation depth, but their modulation speed is expected to be very low ($\ll 1$ kHz), limited by the mechanical alignment of the molecules [73].

Overall, experimental demonstrations of THz modulators/switches so far have always presented severe tradeoffs between insertion loss (IL) and modulation depth. The performance of the electrically driven THz modulators reported in the literature is compared in Fig. 3(a). In terms of a balanced metrics, results reported by Chen *et al.* and Sensale-Rodríguez *et al.* are among the best.

A. Modulators and Switches Based on Large-Area Graphene

In modulators and switches based on traditional semiconductor 2DEGs, the channel carrier concentration is tuned by a metal gate [67], [68], which has been found to impact negatively the device performance in two ways [21]. First, the metal gate introduces a large signal attenuation ($\sim 90\%$ or 10 dB); second, it reduces the modulation depth because of the high gate electrical conductivity in comparison to the highest achievable conductivity of the

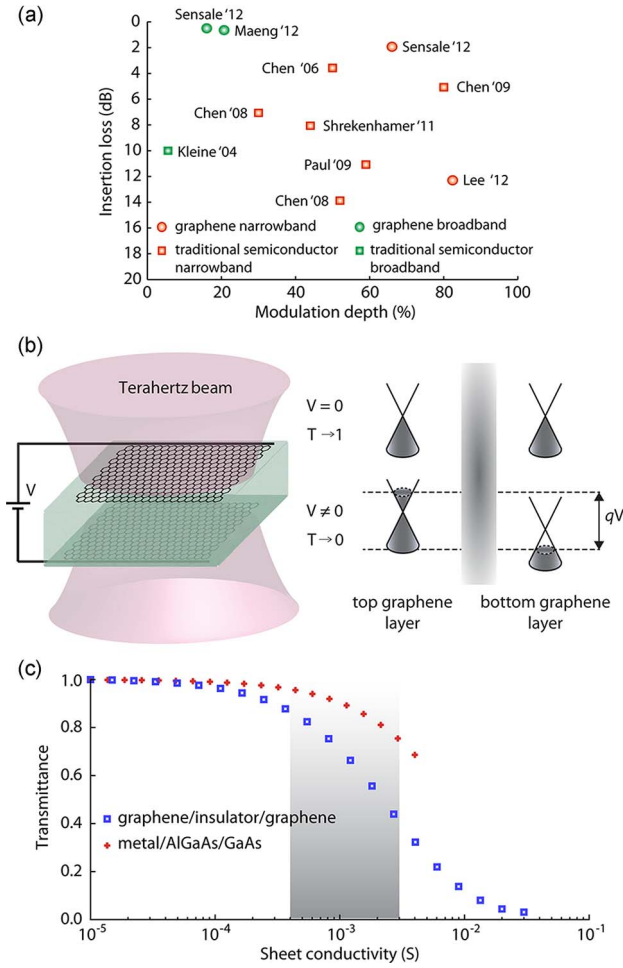


Fig. 3. (a) State of the art of electrically driven THz modulators in terms of modulation depth versus insertion loss. (b) Operation principle of a self-gated graphene pair as THz modulator [21]. By applying a voltage between the two capacitively coupled graphene layers, carriers of the opposite type accumulate in each layer, leading to modulation of conductivity thus THz transmittance. (c) Calculated transmittance for two capacitively coupled 2DEG structures: graphene/insulator/graphene and metal/AlGaAs/GaAs [22]. The transmittance is normalized to the maximum transmission (1-IL) afforded by each structure, which is 95% and 10% for the two structures, respectively.

channel 2DEG. THz power transmittance through a gated 2DEG at normal incidence can be expressed as [21]

$$T_{\text{gate-2DEG}} = 4 / (2 + Z_0(\sigma_{\text{gate}} + \sigma_{2\text{DEG}}))^2 \xrightarrow{\text{with large } \sigma_{\text{gate}}} 0 \quad (4)$$

where the modulation depth (MD) considering a metal gate is given by

$$\text{MD} = 1 - \left[1 + \frac{Z_0 \sigma_{\text{max,2DEG}}}{2 + Z_0 \sigma_{\text{metal}}} \right]^{-2} \xrightarrow{\text{with large } \sigma_{\text{metal}}} 0 \quad (5)$$

where $\sigma_{\text{gate}}/\sigma_{\text{metal}}$ is the gate/metal conductivity, $\sigma_{\text{max,2DEG}}$ is the maximum conductivity achievable in the 2DEG, and Z_0 is the vacuum impedance.

Based on this observation, we have proposed to use graphene/insulator/semiconductor structures as efficient broadband modulators, where graphene with a tunable conductivity acts as an “active gate,” thus reducing loss and increasing modulation depth [21]. An example structure consists of one self-gated graphene pair, as depicted in Fig. 3(b). The principle of operation can be understood as follows: at 0 V, the Fermi level of both graphene layers is at the Dirac point, and, therefore, THz absorption is minimal (transmittance > 95%). When a finite voltage is applied, carriers of opposite types accumulate in each of the capacitively coupled layers, leading to larger optical conductivity, thus reducing transmittance. The modulation depth attainable in such structures depends on the practically achievable conductivity swings in the graphene layers, therefore graphene quality. The insertion loss stems from the minimum conductivity in graphene (~ 0.15 mS [73] at dc, thus IL < 1 dB) [22]. Shown in Fig. 3(c) is the calculated transmittance versus conductivity for graphene/insulator/graphene and metal/AlGaAs/GaAs structures using (4). The transmittance in this figure is normalized with respect to the maximum transmittance of the corresponding structure, which is 95% and 10% for the two structures, respectively. The transmittance is plotted up to the maximum conductivity achievable in the GaAs 2DEGs and graphene [22]. Also shown in Fig. 3(c) is the typical conductivity swing presently achievable in large area graphene, highlighted in gray. It is evident that for the same conductivity swing, the modulation depth is higher in graphene-based modulators than the metal-based ones, which is consistent with the experimental observations.

These structures promise highly efficient and intrinsically broadband modulation for frequencies up to $\omega_0 = 1/\tau$, according to (3). The practical frequency range is thus determined by the substrate and geometry where the intrinsic device is fabricated on. For instance, super broadband operation can be realized using nanomembrane platforms [22].

Recently, this type of intrinsically broadband modulation mechanism was experimentally demonstrated in graphene/SiO₂/Si structures, showing close to 20% modulation depth and IL < 0.5 dB [22], [42]. One of these proof-of-concept devices is sketched in Fig. 4(a), together with a plot of the measured transmittance under two bias conditions after subtracting the substrate effects [solid lines in Fig. 4(b)]. The flat transmittance versus frequency and the excellent agreement with analytical models confirm that the intrinsic device is indeed broadband. The modulation speed in these devices was found to be in the kilohertz to megahertz range, limited by their large RC time constants [22]. The high RC constant is a consequence of the large device area, which needs to be comparable to at least the waist of the THz beam (1.5 mm for the

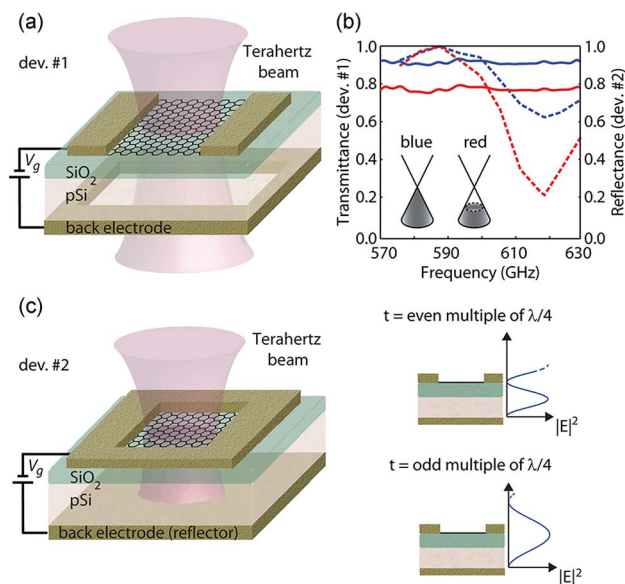


Fig. 4. (a) Sketch of an intrinsically broadband THz beam modulator consisting of a graphene/SiO₂/Si structure (device #1) [22]. (b) Measured THz transmittance/reflectance versus frequency for the transmittance (solid lines, device #1) and reflectance-based (dashed lines, device #2) modulators. (c) Sketch of a reflectance-based THz beam modulator (device #2) consisting of a graphene/SiO₂/Si/metal (reflector) structure [74]. When the substrate thickness is an odd multiple of a quarter wavelength, the electric field intensity is enhanced in the active graphene layer, leading to extraordinary modulation at those frequencies. When the substrate thickness is an even multiple of a quarter wavelength, no modulation is expected.

setup employed in [22]). However, high-speed modulation might be possible by employing alternative structures such as metamaterial devices where the active graphene layers only cover a small fraction of the total device area, or traveling wave approaches so the RC time constant could be circumvented, since the operation speed is set by the local distributed device parameters rather than the lumped total device capacitance and resistance. To enhance modulation depth, the voltage controlled graphene conductivity swing has to be augmented, which can be realized, for example, by employing several stacked capacitively coupled graphene/graphene or graphene/semiconductor pairs [22].

For the given conductivity range presently achievable in large area graphene, another way of improving modulation is to structurally enhance the THz radiation intensity in the active graphene layers, i.e., employing cavities, consequentially with a reduced bandwidth. One simple implementation is reflection-mode devices [74]. An example device structure, as pictured in Fig. 4(c), consists of graphene on top of a p-Si substrate with an optical thickness of an odd multiple of a quarter wavelength and a back metal electrode acting simultaneously as a reflector. A similar structure was also adopted by Lee et al. [75] to demonstrate tuning by graphene in the IR range, though a

small modulation depth of $\sim 4\%$ was obtained since the tunability of absorption in graphene is weak at these frequencies. On the other hand, a very sensitive dependence of absorbance with graphene conductivity can be observed in the THz range, owing to the augmented electric field at the active graphene layer. As shown in Fig. 4(b), while only a $\sim 20\%$ modulation depth is achieved in the previously discussed intrinsically broadband transmittance modulators, the experimentally demonstrated modulation depth in the reflection-mode modulator is around 70%, for an even slightly smaller conductivity swing in graphene. Since the back electrode acts as a reflector, a node of the electric field occurs at the back electrode. Assuming normal incidence, the electric field intensity in the active graphene layer, thus modulation depth, is maximum at frequencies when the substrate optical thickness is an odd multiple of a quarter wavelength. On the contrary, when the substrate optical thickness is an even multiple, the intensity of the electric field at graphene becomes zero, resulting in no modulation. These two situations, pictured in Fig. 4(c), correspond to the cases of antinode and node of the electric field at the active graphene layer, respectively. For the antinode case, four times larger electric field intensity is achieved in comparison to that in the transmittance modulator, thus about four times higher absorption by graphene. In terms of modulation depth versus IL [see Fig. 3(a)], the measured performance of the reflection mode is among the best reported so far among all electrically driven THz modulators.

Another interesting feature of reflection mode devices is that $\sim 100\%$ modulation depth is achievable if graphene conductivity can be tuned to be $\sigma_{dc} = 1/377 \Omega = \sim 2.7 \text{ mS}$. Shown in Fig. 5 is the calculated transmittance/reflectance versus graphene conductivity for the graphene-based transmission/reflection mode THz modulators [76].

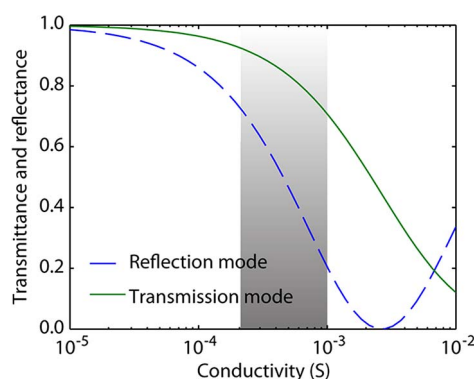


Fig. 5. Calculated transmittance/reflectance versus graphene conductivity for the graphene based transmission/reflection mode THz modulators [76]. It is noteworthy that total THz absorption can be achieved in reflection mode devices. The region highlighted in gray corresponds to a graphene conductivity swing between 0.2 and 1 mS.

The experimentally observed modulation in both transmission and reflection mode devices based on large area graphene corroborates the aforementioned operation principle. When the bias is such that the Fermi level in graphene is at its Dirac point, absorbance is minimal; when a different bias is applied, the Fermi level shifts into conduction/valence band, and thus absorbance increases as the density of states available for intraband transitions is augmented. The modulation speed experimentally achieved in these devices is limited by the large area of the active graphene layer, on the order of kilohertz to megahertz, but it could be increased to gigahertz if metamaterial or traveling wave topologies are adopted. In comparison to the conventional semiconductor-based 2DEGs, graphene offers high hole mobility due to its symmetric band structure, facile integration, thus the possibility of implementing self-gated graphene–graphene/semiconductor pairs with an attractive range of tunable conductivity.

B. Plasmonic Devices

From the previous discussions, we see that the plasmonic effects in graphene are particularly interesting in the frequency range between a few THz to IR, where neither intraband nor interband transitions play dominant roles [see Fig. 1(b)]. Although plasmonics in graphene have been extensively studied from the theoretical point of view, it was not until recently that device applications started to emerge. Plasmonic effects can be utilized in passive structures since complete absorbance of THz/far-IR waves is achievable at the plasmon resonance frequency [44]. For example, in the aforementioned patterned stacks of multiple graphene/insulator layers, $\sim 97\%$ absorbation was achieved at the plasmon resonance frequencies [63]. When these stacked layers are patterned into disks, they behave as polarization-independent notch filters; when they are patterned into ribbons, they behave as polarization-dependent filters or polarizers. While performance of the passive devices is largely similar to metal-based frequency-selective surfaces (FSSs), the unique prospect is tunability of the plasmonic effect in graphene via electric conductivity control. Only very recently, a handful of experimental demonstrations were reported on gate-tunable plasmonic effects: propagating plasmons in large-area graphene in the IR range ($\sim 10 \mu\text{m}$) [54], [55] and localized plasmons in the IR [54] and THz range [43].

Experimental demonstration of field-tunable THz plasmonic devices was reported employing an array of graphene ribbons on SiO_2/Si gated by an ionic gel, whose electrical conductivity is negligible at THz [43] [see Fig. 6(a)]. For a ribbon width of $2 \mu\text{m}$ (with equal inter-ribbon spacings), a shift in the plasmonic peak from 2.7 to 4.2 THz was observed when sweeping gate voltage. The attained absorbation at the plasmon resonance frequency was $\sim 14\%$, larger than the reported values by 2DEGs in traditional semiconductors at room temperature. Upon

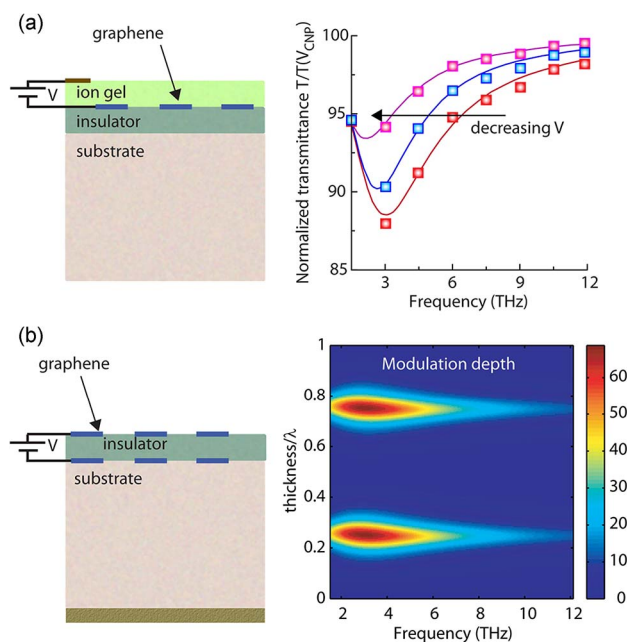


Fig. 6. (a) *Left: Structure of the field-tunable THz plasmonic device reported in [43]. Right: Its measured transmittance versus frequency showing gate-tuned plasmonic absorption in the graphene ribbons. Data are extracted from [43] for a ribbon width of $4 \mu\text{m}$.* (b) *Left: Sketch of a proposed plasmonic THz modulator with a reflector on the back in order to enhance electric field at the graphene active layers [78]. Right: Simulated modulation depth versus frequency for different substrate thicknesses. When the substrate thickness is odd multiple of a quarter wavelength at the resonance of the plasmonic structure, the modulation depth can approach 70% for the geometry and material parameters reported for the active device component shown in (a).*

more careful analysis, the higher absorption by graphene is attributed to the more favorable dielectric environment (lower permittivity) in the graphene device than that which supports high mobility 2DEGs in traditional semiconductors [46], [62], [77]. Transmittance through graphene on a thick substrate is given by (when considering the first pass only as can be measured by THz time-domain spectroscopy)

$$T = \frac{1}{|1 + Z_0\sigma(\omega)/(1 + n_{\text{sub}})|^2} \quad (6)$$

where n_{sub} is the substrate refractive index at THz. Since we can choose substrates with low refractive index to support the active graphene elements, plasmonic resonance in graphene can be stronger than a 2DEG in conventional semiconductors for the same conductivity. This is one of the unique and key attributes of graphene owing to its 2-D nature.

To design for practical THz applications, it is imperative to overcome the low absorption by a single-layer

graphene that is limited by its low maximum dc conductivity currently achievable. For instance, by stacking several self-gated graphene pairs, the strength of the plasmonic absorption and peak tunability can be greatly enhanced. Moreover, to design tunable plasmonic structures for a fixed frequency, cavities can be employed to concentrate the electromagnetic energy at the active graphene region. Let us use the reflection modulation platform discussed previously again as an example. The sketch of such a structure and predicted modulation depth are shown in Fig. 6(b) [78]. A ribbon width of 4 μm along with other material parameters reported in [39] is assumed, corresponding to a plasmonic resonance near 3 THz. Simulations show that the modulation can reach 70% for the same dc conductivity swing as reported in [43], when the substrate thickness is matched to an odd multiple of a quarter wavelength of the plasmonic resonance frequency [78].

In short, tunable plasmonic effects in patterned graphene can potentially enable promising solutions in the frequency range where the Drude conductivity falls off and interband transitions are low: $1/\tau < \omega < E_f/\hbar$, E_f being the Fermi level in graphene measured from the Dirac point. The unique attribute of graphene devices is that plasmonic effects can be augmented by dielectric engineering, which might not be easy for conventional semiconductors.

C. Graphene THz Metamaterials

In Section III-A, we discussed that electromagnetic field can be concentrated by cavities, therefore higher modulation can be achieved for a given conductivity range. Metamaterials or FSSs can be viewed as one type of cavities, which are composed of artificially engineered subwavelength units or meta-atoms, thus yielding properties unattainable in natural materials [79]. When combined with tunable elements such as graphene self-gated pairs, it is possible to realize reconfigurable metamaterials [80], [81].

Interaction of graphene layers with metallic or dielectric FSSs, i.e., in a graphene metamaterial configuration, was first studied in the mid-IR range [82]. It was found that the transmittance versus frequency characteristic of a photonic metamaterial shifted when placing graphene on top, because of the electromagnetic interaction between the conductive graphene and the passive photonic structure. Since adsorbates on graphene change the electrical properties of graphene, these structures have been proposed as molecule sensors [82], [83].

The scheme in Chen’s tunable THz metamaterials—GaAs gated by a metallic FSS (Schottky junction)—was also recently adopted for graphene [84]. Lee *et al.* employed periodic arrays of metallic hexagonal and asymmetric double split circular rings as meta-atoms of the THz FSS, and transferred graphene directly onto the metallic FSSs (see Fig. 7(a) reproduced from [84]). Since it is

impossible to use these FSSs to apply dc bias to gate graphene (the circular meta-atoms are isolated from each other), Lee *et al.* utilized another THz FSS made of an array of metal wires as the gate, which is separated from graphene using a polymer layer as the insulator. By sweeping the voltage between the metal wire FSS and graphene sheet, intensity modulation depths of 72% and 49% were experimentally observed for a single-layer graphene on top of the hexagonal and double split circular ring FSSs, respectively. When employing multilayer graphene, 82%

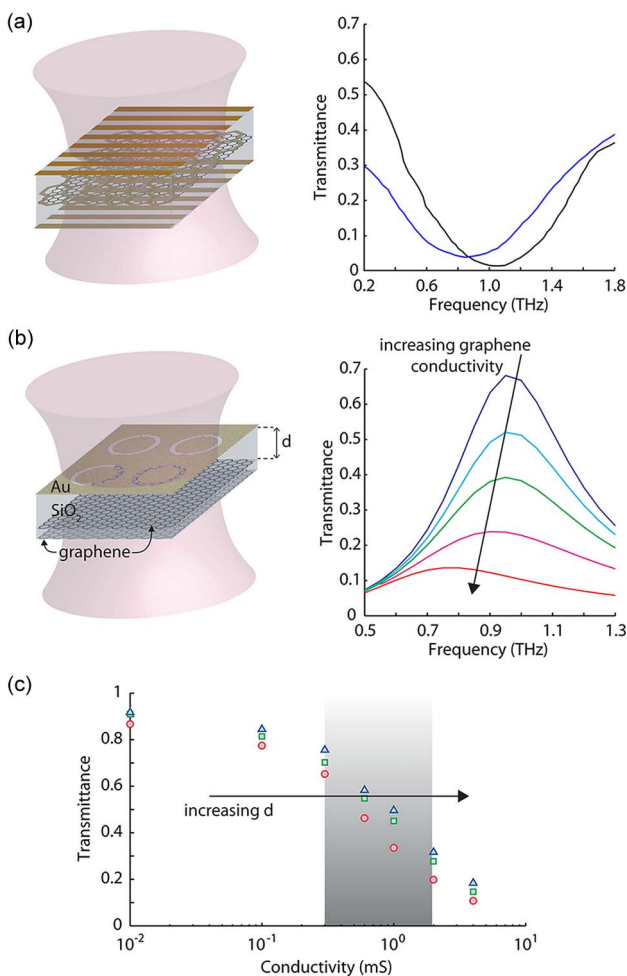


Fig. 7. (a) Sketch of the graphene metamaterial THz modulator reported in [84], and its performance in terms of transmittance versus frequency for the maximum voltage swing applied; the plot is reproduced from [84]. (b) Sketch of a metamaterial THz modulator employing a ring slot FSS and two self-gated graphene layers as the active element; transmittance versus graphene conductivity is simulated showing 85% modulation depth and less than 2-dB loss for a conductivity swing typical in normal quality large area graphene. (c) Transmittance versus conductivity at the structure resonance frequency for different separation d between the FSS and the active graphene layers. Shown in gray is the typical conductivity swing achievable in the graphene pair. There is an optimal placement with maximized modulation depth. This observation is also valid for other FSS such as cross slot [80].

modulation was achieved. However, the large relative change of transmission ($MD = |T - T_0|/T_0$) was obtained on the expense of very high insertion loss ($IL = 1 - T_0$): for all the cases > 12 dB or $\sim 95\%$. This is most likely because graphene is right on top of the metallic FSS, and perhaps also due to the low-Q (quality factor) of the FSSs employed.

When integrating graphene with metamaterials or FSSs with larger Q, one can obtain greater enhancement of the tunability afforded by graphene. We recently proposed an alternative approach [80]: employing self-gated 2DEG pairs as the tunable element, and consequently optimizing the placement of the active element from the FSSs. An example of such a THz metamaterial modulator structure employing ring slot FSSs is pictured in Fig. 7(b). The active tuning of graphene conductivity is achieved in two capacitively coupled graphene layers. When increasing (decreasing) the distance between the active element and FSS, the transmittance versus conductivity curve shifts toward right (left) along the conductivity axis, as shown in Fig. 7(c). Therefore, there is an optimal placement for the active graphene layers that renders an optimal tradeoff between modulation depth and IL. When the active element is placed at this distance, our simulations show that close to 85% MD with simultaneously low loss (smaller than 2 dB) is achievable.

Based on the same principle, reconfigurable multiband filters can be constructed. This mechanism can also be readily extended to other FSSs as well as other frequency ranges. The key attribute of our proposed tunable metamaterials hinges on self-gated 2DEGs, which are relatively easy to realize using graphene/graphene or graphene/traditional semiconductors.

IV. TOWARD FUTURE DEVICES AND SYSTEMS

The graphene-based reconfigurable THz devices presented here can be easily integrated with other THz devices to increase functionality or to realize single chip THz systems. For instance, as reported by Sensale-Rodríguez et al. [85], arrays of graphene electroabsorption modulators can be employed as electrically reconfigurable patterns for terahertz cameras. Future developments in graphene-

based modulators and the use of advanced imaging algorithms such as coded aperture [86], might promise exceptional system performance. Modulation of reflection by large area graphene layers was also theoretically proposed for THz cloaking [87], which can now be experimentally demonstrated based on the performance achieved in reflection-based modulators [74]. In addition to reconfigurable filters, modulators and switches, polarizers, and sensors, graphene has been recently demonstrated to allow for THz emission and detection [88]–[95]. Integration of THz modulators with detectors might lead to low-power on-chip THz transceivers.

However, substantial number of challenges remains to improve the experimental performance of these devices. For instance, it is imperative to improve the quality of large-area graphene in terms of high mobility and uniformity. Self-gated 2DEG pairs with favorable band alignment still need to be fabricated with minimal adverse effects from traps.

V. CONCLUSION

Tunable THz optical properties of graphene, together with its ease of fabrication and integration, enable us to construct efficient and novel THz reconfigurable devices. In particular, active modulators using graphene have been demonstrated, based on the Drude/plasmonic behavior, or metamaterials. These devices exhibit performance comparable to the state of the art built on conventional materials, which is remarkable, given that graphene is only one atom thick. Harvesting graphene and related materials for THz is still at its very early stage. It is unavoidable that some interesting studies related to reconfigurable THz optoelectronics are not discussed in this paper since the field is blooming quickly. The work described in this paper presents only the first steps to develop promising solutions using graphene for THz technologies. ■

Acknowledgment

The authors would like to thank T. Fang, K. Tahy, W. S. Hwang, M. Kelly, A. Seabaugh, P. Fay, and S. J. Allen for useful discussions.

REFERENCES

- [1] P. H. Siegel, "Terahertz technology," *IEEE Trans. Microw. Theory Tech.*, vol. 50, no. 3, pp. 910–928, Mar. 2002.
- [2] M. Tonouchi, "Cutting edge terahertz technology," *Nature Photon.*, vol. 1, pp. 97–105, 2007.
- [3] B. Ferguson and X. C. Zhang, "Materials for terahertz science and technology," *Nature Mater.*, vol. 1, pp. 26–33, 2002.
- [4] H. T. Chen, W. J. Padilla, J. M. O. Zide, A. C. Gossard, A. J. Taylor, and R. D. Averitt, "Active terahertz metamaterial devices," *Nature*, vol. 444, pp. 597–600, 2006.
- [5] D. A. Crawley, C. Longbottom, B. E. Cole, C. M. Ciesla, D. Arnone, V. P. Wallace, and M. Pepper, "Terahertz pulse imaging: A pilot study of potential applications in dentistry," *Caries Res.*, vol. 37, no. 5, pp. 352–359, 2003.
- [6] A. J. Fitzgerald, V. P. Wallace, M. Jimenez-Linan, L. Bobrow, R. J. Pye, A. D. Purushotham, and D. D. Arnone, "Terahertz pulsed imaging of human breast tumour," *Radiology*, vol. 239, pp. 533–540, 2006.
- [7] R. Wallace and H. B. Appleby, "Standoff detection of weapons and contraband in the 100 GHz to 1 THz region," *IEEE Trans. Antennas Propag.*, vol. 55, no. 11, pp. 2944–2956, Nov. 2007.
- [8] A. J. Fitzgerald, E. Berry, N. N. Zinovev, G. C. Walker, M. A. Smith, and J. M. Chamberlain, "An introduction to medical imaging with coherent terahertz frequency radiation," *Phys. Med. Biol.*, vol. 47, no. 7, pp. R67–R84, 2002.
- [9] J. F. O'Hara, W. Withayachumnankul, and I. Al-Naib, "A review on thin-film sensing with terahertz waves," *J. Infrared Millimeter*

- Terahertz Waves*, vol. 33, no. 3, pp. 245–291, 2012.
- [10] T. R. Globus, D. L. Woolard, T. Khromova, T. W. Crowe, M. Bykhovskaia, B. L. Gelmont, J. Hesler, and A. C. Samuels, “THz-spectroscopy of biological molecules,” *J. Biol. Phys.*, vol. 29, no. 2/3, pp. 89–100, 2003.
- [11] A. Dobroui, Y. Sasaki, T. Shibuya, C. Otani, and K. Kawase, “THz-wave spectroscopy applied to the detection of illicit drugs in mail,” *Proc. IEEE*, vol. 95, no. 8, pp. 1566–1575, Aug. 2007.
- [12] L. Moeller, J. Federici, and K. Su, “2.5 Gbit/s duobinary signalling with narrow bandwidth 0.625 terahertz source,” *Electron. Lett.*, vol. 47, pp. 856–858, 2011.
- [13] T. Kleine-Ostmann and T. Nagatsuma, “A review on terahertz communications research,” *J. Infrared Millimeter Terahertz Waves*, vol. 32, no. 2, pp. 143–171, 2011.
- [14] J. Federici and L. Moeller, “Review of terahertz and subterahertz wireless communications,” *J. Appl. Phys.*, vol. 107, no. 11, 2010, 111101.
- [15] J. M. Fitch and R. Osiander, “Terahertz waves for communications and sensing,” *Johns Hopkins APL Tech. Dig.*, vol. 25, no. 4, pp. 348–355, 2004.
- [16] T. Kleine-Ostmann, M. Koch, and P. Dawson, “Modulation of THz radiation by semiconductor nanostructures,” *Microw. Opt. Technol. Lett.*, vol. 35, no. 5, pp. 343–345, 2002.
- [17] H. T. Chen, J. F. O’Hara, A. K. Azad, A. J. Taylor, R. D. Averitt, D. B. Shrekenhamer, and W. J. Padilla, “Experimental demonstration of frequency-agile terahertz metamaterials,” *Nature Photon.*, vol. 2, pp. 295–298, 2008.
- [18] D. Shrekenhamer, S. Rout, A. Strikwerda, C. Bingham, R. Averitt, S. Sonkusale, and W. Padilla, “High speed terahertz modulation from metamaterials with embedded high electron mobility transistors,” *Opt. Exp.*, vol. 19, pp. 9968–9975, 2011.
- [19] C. W. Berry, J. Moore, and M. Jarrahi, “Design of reconfigurable metallic slits for terahertz beam modulation,” *Opt. Exp.*, vol. 19, no. 2, pp. 1236–1245, 2011.
- [20] C. Liu, J. Ye, and Y. Zhang, “Thermally tunable THz filter made of semiconductors,” *Opt. Commun.*, vol. 283, pp. 865–868, 2010.
- [21] B. Sensale-Rodríguez, T. Fang, R. Yan, M. M. Kelly, D. Jena, L. Liu, and H. G. Xing, “Unique prospects for graphene-based terahertz modulators,” *Appl. Phys. Lett.*, vol. 99, 2011, 113104.
- [22] B. Sensale-Rodríguez, R. Yan, M. M. Kelly, T. Fang, K. Tahy, W. S. Hwang, D. Jena, L. Liu, and H. G. Xing, “Broadband graphene terahertz modulators enabled by intraband transitions,” *Nature Commun.*, vol. 3, 2012, 780.
- [23] K. S. Novoselov, A. K. Geim, S. V. Morozov, D. Jiang, Y. Zhang, S. V. Dubonos, I. V. Grigorieva, and A. A. Firsov, “Electric field effect in atomically thin carbon films,” *Science*, vol. 306, pp. 666–669, 2004.
- [24] Y. M. Lin, A. V. Garcia, S. J. Han, D. B. Farmer, I. Meric, Y. Sun, Y. Wu, C. Dimitrakopoulos, A. Grill, P. Avouris, and K. A. Jenkins, “Wafer-scale graphene integrated circuit,” *Science*, vol. 332, no. 6035, pp. 1294–1297, 2011.
- [25] F. Bonaccorso, Z. Sun, T. Hasan, and A. C. Ferrari, “Graphene photonics and optoelectronics,” *Nature Photon.*, vol. 4, no. 9, pp. 611–622, 2010.
- [26] J. Dawlaty et al., “Measurement of the optical absorption spectra of epitaxial graphene from terahertz to visible,” *App. Phys. Lett.*, vol. 93, 2008, 131905.
- [27] L. A. Falkovsky, “Optical properties of graphene,” *J. Phys., Conf. Ser.*, vol. 129, 2008, 012004.
- [28] T. Ando, Y. Zheng, and H. Suzuura, “Dynamical conductivity and zero-mode anomaly in honeycomb lattices,” *J. Phys. Soc. Jpn.*, vol. 71, no. 5, pp. 1318–1324, 2002.
- [29] R. R. Nair, P. Blake, A. N. Grigorenko, K. S. Novoselov, T. J. Booth, T. Stauber, N. M. R. Peres, and A. K. Geim, “Fine structure constant defines visual transparency of graphene,” *Science*, vol. 320, p. 1308, 2008.
- [30] K. S. Kim, Y. Zhao, H. Jang, S. Y. Lee, J. M. Kim, K. S. Kim, J.-H. Ahn, P. Kim, J.-Y. Choi, and B. H. Hong, “Large-scale pattern growth of graphene films for stretchable transparent electrodes,” *Nature*, vol. 457, pp. 706–710, 2009.
- [31] Z. Q. Li, E. A. Henriksen, Z. Jiang, Z. Hao, M. C. Martin, P. Kim, H. L. Stormer, and D. N. Basov, “Dirac charge dynamics in graphene by infrared spectroscopy,” *Nature Phys.*, vol. 4, pp. 532–535, 2008.
- [32] F. Wang, Y. Zhang, C. Tian, C. Giri, A. Zettl, M. Crommie, and Y. R. Shen, “Gate-variable optical transitions in graphene,” *Science*, vol. 320, no. 5876, pp. 206–209, 2008.
- [33] Z. P. Sun, T. Hasan, F. Torrisi, D. Popa, G. Privitera, F. Q. Wang, F. Bonaccorso, D. M. Basko, and A. C. Ferrari, “Graphene mode-locked ultrafast laser,” *ACS Nano*, vol. 4, no. 2, pp. 803–810, 2010.
- [34] M. Liu, X. Yin, E. Ulin-Avila, B. Geng, T. Zentgraf, L. Ju, F. Wang, and X. Zhang, “A graphene-based broadband optical modulator,” *Nature*, vol. 474, pp. 64–67, 2011.
- [35] M. Liu, X. Yin, and X. Zhang, “Double-layer graphene optical modulator,” *Nano Lett.*, vol. 12, no. 3, pp. 1482–1485, 2012.
- [36] S. J. Koester and M. Li, “High-speed waveguide-coupled graphene-on-graphene optical modulators,” *Appl. Phys. Lett.*, vol. 100, 2012, 171107.
- [37] V. Ryzhii, T. Otsuji, M. Ryzhii, V. G. Leiman, S. O. Yurchenko, V. Mitin, and M. S. Shur, “Effect of plasma resonances on dynamic characteristics of double graphene-layer optical modulator,” *J. Appl. Phys.*, vol. 112, 2012, 104507.
- [38] S. Kola, J. M. Golio, and G. N. Maracas, “An analytical expression for Fermi level versus sheet carrier concentration for HEMT modeling,” *IEEE Electron Device Lett.*, vol. EDL-9, no. 3, pp. 136–138, Mar. 1988.
- [39] T. Fang, A. Konar, H. Xing, and D. Jena, “Carrier statistics and quantum capacitance of graphene sheets and ribbons,” *Appl. Phys. Lett.*, vol. 91, no. 9, 2007, 092109.
- [40] L. A. Falkovsky and S. S. Pershoguba, “Optical far-infrared properties of a graphene monolayer and multilayer,” *Phys. Rev. B*, vol. 76, 2007, 153410.
- [41] J. Horng, C.-F. Chen, B. Geng, C. Girit, Y. Zhang, Z. Hao, H. A. Bechtel, M. Martin, A. Zettl, M. F. Crommie, Y. R. Shen, and F. Wang, “Drude conductivity of Dirac fermions in graphene,” *Phys. Rev. B*, vol. 83, 2011, 165113.
- [42] I. Maeng, S. C. Lima, S. J. Chae, Y. H. Lee, H. Choi, and J. H. Son, “Gate-controlled nonlinear conductivity of Dirac fermion in graphene field-effect transistors measured by terahertz time-domain spectroscopy,” *Nano Lett.*, vol. 12, pp. 551–555, 2012.
- [43] L. Jua, B. Geng, J. Horng, C. Girit, M. Martin, Z. Hao, H. A. Bechtel, X. Liang, A. Zettl, Y. R. Shen, and F. Wang, “Graphene plasmonics for tunable terahertz metamaterials,” *Nature Nanotechnol.*, vol. 6, pp. 630–634, 2011.
- [44] S. Thongrattanasiri, F. H. Koppens, and F. J. Garcia de Abajo, “Complete optical absorption in periodically patterned graphene,” *Phys. Rev. Lett.*, vol. 108, 2012, 047401.
- [45] R. H. Ritchie, “Plasma losses by fast electrons in thin films,” *Phys. Rev.*, vol. 106, pp. 874–881, 1957.
- [46] S. J. Allen, D. C. Tsui, and R. A. Logan, “Observation of the two-dimensional plasmon in silicon inversion layers,” *Phys. Rev. Lett.*, vol. 38, pp. 980–983, 1977.
- [47] W. A. Murray and W. L. Barnes, “Plasmonic materials,” *Adv. Mater.*, vol. 19, no. 22, pp. 3771–3782, 2007.
- [48] B. Wunsch, T. Stauber, F. Sols, and F. Guinea, “Dynamical polarization of graphene at finite doping,” *New J. Phys.*, vol. 8, 2006, DOI: 10.1088/1367-2630/8/12/318.
- [49] O. Vafek, “Thermoplasma polariton within scaling theory of single-layer graphene,” *Phys. Rev. Lett.*, vol. 97, 2006, 266406.
- [50] L. Brey and H. A. Fertig, “Elementary electronic excitations in graphene nanoribbons,” *Phys. Rev. B*, vol. 75, 2007, 125434.
- [51] E. H. Hwang and S. Das Sarma, “Dielectric function, screening, and plasmons in 2D graphene,” *Phys. Rev. B*, vol. 75, 2007, 205418-1.
- [52] S. Das Sarma and E. H. Hwang, “Collective modes of the massless Dirac plasma,” *Phys. Rev. Lett.*, vol. 102, 2009, 206412.
- [53] E. H. Hwang and S. Das Sarma, “Plasmon modes of spatially separated double layer graphene,” *Phys. Rev. B*, vol. 80, 2009, 205405.
- [54] J. Chen, M. Badioli, P. Alonso-González, S. Thongrattanasiri, F. Huth, J. Osmond, M. Spasenovic, A. Centeno, A. Pesquera, P. Godignon, A. Zurutuza, N. Camara, J. Garcia de Abajo, R. Hillenbrand, and F. Koppens, “Optical nanoimaging of gate-tunable graphene plasmons,” *Nature*, vol. 487, pp. 77–81, 2012.
- [55] Z. Feia, A. S. Rodin, G. O. Andreeva, W. Bao, A. S. McLeod, M. Wagner, L. M. Zhang, Z. Zhao, G. Dominguez, M. Thiemens, M. M. Fogler, A. H. Castro-Neto, C. N. Lau, F. Keilmann, and D. N. Basov, “Gate-tuning of graphene plasmons revealed by infrared nano-imaging,” *Nature*, vol. 487, pp. 72–85, 2012.
- [56] V. Ryzhii, “Terahertz plasma waves in gated graphene heterostructures,” *Jpn. J. Appl. Phys.*, vol. 45, 2006, L923.
- [57] V. Ryzhii, A. Satou, and T. Otsuji, “Plasma waves in two-dimensional electron-hole system in gated graphene heterostructures,” *J. Appl. Phys.*, vol. 101, 2007, 024509.
- [58] F. Rana, “Graphene terahertz plasmon oscillators,” *IEEE Trans. Nanotechnol.*, vol. 7, no. 1, pp. 91–99, Jan. 2008.
- [59] V. M. Shalaev, “Electromagnetic properties of small-particle composites,” *Phys. Rep.*, vol. 272, no. 2–3, pp. 61–137, 1996.

- [60] D. A. Genov, A. K. Sarychev, V. M. Shalaev, and A. Wei, "Resonant field enhancement from metal nanoparticle arrays," *Nano Lett.*, vol. 4, pp. 153–158, 2004.
- [61] W. R. Frensley, "High-frequency effects of ballistic electron transport in semiconductors," *IEEE Electron Device Lett.*, vol. EDL-1, no. 7, pp. 137–139, Jul. 1980.
- [62] S. J. Allen, H. L. Stormer, and J. C. M. Hwang, "Dimensional resonance of the two-dimensional electron gas in selectively doped GaAs/AlGaAs heterostructures," *Phys. Rev. B*, vol. 28, pp. 4875–4877, 1983.
- [63] H. Yan, X. Li, B. Chandra, G. Tulevski, Y. Wu, M. Freitag, W. Zhu, P. Avouris, and F. Xia, "Tunable infrared plasmonic devices using graphene/insulator stacks," *Nature Nanotechnol.*, vol. 7, pp. 330–334, 2012.
- [64] H. Chen, H. Lu, A. Azad, R. Averitt, A. Gossard, S. Trugman, J. O'Hara, and A. Taylor, "Electronic control of extraordinary terahertz transmission through subwavelength metal hole arrays," *Opt. Exp.*, vol. 16, pp. 7641–7648, 2008.
- [65] O. Paul, C. Imhof, B. Lägela, S. Wolff, J. Heinrich, S. Höfling, A. Forchel, R. Zengerle, R. Beigang, and M. Rahm, "Polarization-independent active metamaterial for high-frequency terahertz modulation," *Opt. Exp.*, vol. 17, no. 2, pp. 819–827, 2009.
- [66] H. T. Chen, W. J. Padilla, M. J. Cich, A. K. Azad, R. D. Averitt, and A. J. Taylor, "A metamaterial solid-state terahertz phase modulator," *Nature Photon.*, vol. 3, pp. 141–151, 2009.
- [67] T. Kleine-Ostmann, P. Dawson, K. Pierz, G. Hein, and M. Koch, "Room-temperature operation of an electrically driven terahertz modulator," *Appl. Phys. Lett.*, vol. 84, no. 18, 2004, DOI: <http://dx.doi.org/10.1063/1.1723689>.
- [68] T. Kleine-Ostmann, K. Pierz, G. Hein, P. Dawson, M. Marso, and M. Koch, "Spatially resolved measurements of depletion properties of large gate two dimensional electron gas semiconductor terahertz modulators," *J. Appl. Phys.*, vol. 205, 2009, 093707.
- [69] P. Kuzel, F. Kadlec, J. Petzelt, J. Schubert, and G. Panaitov, "Highly tunable SrTiO₃/DyScO₃ heterostructures for applications in the terahertz range," *Appl. Phys. Lett.*, vol. 91, no. 23, 2007, 232911.
- [70] H. Nemeč, P. Kuzel, L. Duvillaret, A. Pashkin, M. Dressel, and M. T. Sebastian, "Highly tunable photonic crystal filter for the terahertz range," *Opt. Lett.*, vol. 30, no. 5, pp. 549–551, Mar. 2005.
- [71] Y. S. Kim, S. Y. Lin, H. Y. Wu, and R. P. Pan, "A tunable terahertz filter and its switching properties in terahertz region based on a defect mode of a metallic photonic crystal," *J. Appl. Phys.*, vol. 109, pp. 123 111–123 114, 2011.
- [72] N. Vieweg, N. Born, I. Al-Naib, and M. Koch, "Electrically tunable terahertz notch filters," *J. Infrared Millimeter Terahertz Waves*, vol. 33, pp. 327–332, 2012.
- [73] N. M. R. Peres and T. Stauber, "Transport in a clean graphene sheet at finite temperature and frequency," *Int. J. Mod. Phys. B*, vol. 22, pp. 2529–2536, 2008.
- [74] B. Sensale-Rodríguez, R. Yan, S. Rafique, M. Zhu, W. Li, X. Liang, D. Gundlach, V. Protasenko, M. M. Kelly, D. Jena, L. Liu, and H. G. Xing, "Extraordinary control of terahertz beam reflectance in graphene electro-absorption modulators," *Nano Lett.*, vol. 12, no. 9, pp. 4518–4522, 2012.
- [75] C.-C. Lee, S. Suzuki, W. Xie, and T. R. Schibli, "Broadband graphene electro-optic modulators with sub-wavelength thickness," *Opt. Exp.*, vol. 20, no. 5, pp. 5264–5269, 2012.
- [76] B. Sensale-Rodríguez, R. Yan, S. Rafique, M. Zhu, M. Kelly, V. Protasenko, D. Jena, L. Liu, and H. G. Xing, "Exceptional tunability of THz reflectance in graphene structures," in *Proc. 37th Int. Conf. Infrared Millimeter Terahertz Waves*, 2012, DOI: 10.1109/IRMMW-THz.2012.6380082.
- [77] H. Zhang, M. Zhu, B. Sensale-Rodríguez, and H. G. Xing, "THz plasmonic absorption in periodically patterned semiconductor ribbons," in *Proc. IEEE Int. Wireless Symp.*, 2013, to be published.
- [78] B. Sensale-Rodríguez, R. Yan, M. Zhu, D. Jena, L. Liu, and H. G. Xing, "Efficient terahertz electro-absorption modulation employing graphene plasmonic structures," *Appl. Phys. Lett.*, vol. 101, no. 26, 2012, 261115.
- [79] N. I. Zheludev, "The road ahead for metamaterials," *Science*, vol. 328, pp. 582–583, 2010.
- [80] R. Yan, B. Sensale-Rodríguez, L. Liu, D. Jena, and H. G. Xing, "A new class of tunable metamaterial terahertz modulators," *Opt. Exp.*, vol. 20, no. 27, pp. 28664–28671, 2012.
- [81] N. Zheludev, "A roadmap for metamaterials," *Opt. Photon. News*, vol. 22, no. 3, pp. 30–35, 2011.
- [82] N. Papanikolaou, Z. Luo, Z. Shen, F. De Angelis, E. Di Fabrizio, A. Nikolaenko, and N. Zheludev, "Graphene in a photonic metamaterial," *Opt. Exp.*, vol. 18, no. 8, pp. 8353–8359, 2010.
- [83] N. Rangel and J. M. Seminario, "Vibronics and plasmonic graphene based sensors," *J. Chem. Phys.*, vol. 132, 2010, 125102.
- [84] S. H. Lee, M. Choi, T.-T. Kim, S. Lee, M. Liu, X. Yin, H. K. Choi, S. S. Lee, C.-G. Choi, S.-Y. Choi, X. Zhang, and B. Min, "Switching terahertz waves with gate-controlled active graphene metamaterials," *Nature Mater.*, vol. 11, pp. 936–941, 2012.
- [85] B. Sensale-Rodríguez, S. Rafique, R. Yan, M. Zhu, D. Jena, L. Liu, and H. G. Xing, "Terahertz imaging employing graphene modulator arrays," *Opt. Exp.*, vol. 21, no. 2, pp. 2324–2330, 2013.
- [86] W. L. Chan, K. Charan, D. Takhar, K. F. Kelly, R. G. Baraniuk, and D. M. Mittleman, "A single-pixel terahertz imaging system based on compressed sensing," *Appl. Phys. Lett.*, vol. 93, 2008, 121105.
- [87] P. Y. Chen and A. Alu, "Atomically thin surface cloak using graphene monolayers," *ACS Nano*, vol. 5, no. 7, pp. 5855–5863, 2011.
- [88] V. Ryzhii, M. Ryzhii, N. Ryabova, V. Mitin, and T. Otsuji, "Graphene nanoribbon phototransistor: Proposal and analysis," *Jap. J. Appl. Phys.*, vol. 48, 2009, 04C144.
- [89] V. Ryzhii, M. Ryzhii, N. Ryabova, V. Mitin, and T. Otsuji, "Terahertz and infrared detectors based on graphene structures," *Infrared Phys. Technol.*, vol. 54, pp. 302–305, 2011.
- [90] L. Vicarelli, M. S. Vitiello, D. Coquillat, A. Lombardo, A. C. Ferrari, W. Knap, M. Polini, V. Pellegrini, and A. Tredicucci, "Graphene field effect transistors as room-temperature terahertz detectors," *Nature Mater.*, vol. 11, pp. 865–871, 2012.
- [91] V. Ryzhii, M. Ryzhii, and T. Otsuji, "Negative dynamic conductivity of graphene with optical pumping," *J. Appl. Phys.*, vol. 101, 2007, 083114.
- [92] S. Boubanga-Tombet, S. Chan, T. Watanabe, A. Satou, V. Ryzhii, and T. Otsuji, "Ultrafast carrier dynamics and terahertz emission in optically pumped graphene at room temperature," *Phys. Rev. B*, vol. 85, 2012, 035443.
- [93] T. Otsuji, S. Boubanga-Tombet, A. Satou, M. Suemitsu, and V. Ryzhii, "Spectroscopic study on ultrafast carrier dynamics and terahertz amplified stimulated emission in optically pumped graphene," *J. Infrared Millimeter Terahertz Waves*, vol. 33, pp. 825–838, 2012.
- [94] L. Prechtel, L. Song, D. Schuh, P. Ajayan, W. Wegscheider, and A. W. Holleitner, "Time-resolved ultrafast photocurrents and terahertz generation in freely suspended graphene," *Nature Commun.*, vol. 3, 2012, DOI: 10.1038/ncomms1656.
- [95] J. Yan, M.-H. Kim, J. A. Elle, A. B. Sushkov, G. S. Jenkins, H. M. Milchberg, M. S. Fuhrer, and H. D. Drew, "Dual-gated bilayer graphene hot electron bolometer," *Nature Nano.*, vol. 7, pp. 472–478, 2012.

ABOUT THE AUTHORS

Berardi Sensale-Rodríguez (Student Member, IEEE) received the Engineer's degree from the Universidad de la República, Montevideo, Uruguay, in 2008 and the Ph.D. degree from the University of Notre Dame, Notre Dame, IN, USA, in 2013.

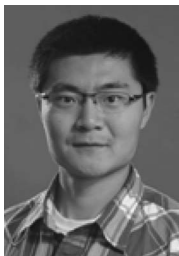
His early research interests were focused on numerical modeling of radio-frequency (RF)/microwave components and analog circuit design oriented toward low-power (subthreshold) portable and implantable electronics. His doctoral work



at Notre Dame was focused on the proposal and development of novel terahertz devices and systems. More recent interests include optoelectronic devices. He has authored/coauthored over 30 research articles in these and related areas.

Dr. Sensale-Rodríguez is a member of the International Society for Optics and Photonics (SPIE) and the American Physical Society (APS), and an associate member of the Uruguayan National Researchers System (SNI). He is the recipient of the Best Student Paper Award from the 2012 International Conference on Infrared, Millimeter, and Terahertz Waves.

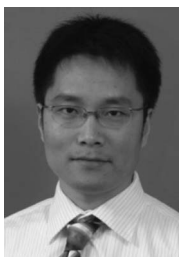
Rusen Yan received the B.S. degree in optoelectronics from Shandong University, Jinan, Shandong, China, in 2010, where he worked on image reconstruction based on generalized phase-shifting interferometry under the advice of Prof. L. Cai. He also received the M.S. degree in electrical engineering from the University of Notre Dame, Notre Dame, IN, USA, in 2011, where he is currently working toward the Ph.D. degree under the advice of Prof. H. G. Xing.



He has authored/coauthored 11 journal articles and seven conference talks. Since June 2010, he has been focused on the development of graphene-based optoelectronic devices as well as investigating the fundamental properties of various 2-D crystals using optical methods.

Mr. Yan is a member of the Optical Society of America (OSA), the International Society for Optics and Photonics (SPIE), and the American Physical Society (APS).

Lei Liu (Member, IEEE) received the B.S. and M.S. degrees in electrical engineering from Nanjing University, Nanjing, China, in 1998 and 2001, respectively, and the Ph.D. degree in electrical engineering from the University of Virginia, Charlottesville, VA, USA, in 2007.



From 2007 to 2009, he was a Postdoctoral Research Associate with the Department of Electrical and Computer Engineering, University of Virginia. In September 2009, he joined the faculty of the University of Notre Dame, Notre Dame, IN, USA, where he is now an Assistant Professor of Electrical Engineering. His research interests include millimeter- and submillimeter-wave device and circuit design, modeling, and testing, quasi-optical techniques, terahertz detectors for imaging and spectroscopy, novel microwave materials and devices, superconducting electronics, microfabrication, and processing.

Debdeep Jena (Member, IEEE) received the B.Tech. degree with a major in electrical engineering and a minor in physics from the Indian Institute of Technology, Kanpur, India, in 1998 and the Ph.D. degree in electrical and computer engineering from the University of California Santa Barbara, Santa Barbara, CA, USA, in 2003.



Since 2003, he has been with the faculty of the Department of Electrical Engineering, University of Notre Dame, Notre Dame, IN, USA. His research and teaching interests are in the MBE growth and device applications of quantum semiconductor heterostructures (currently III-V nitride semiconductors); investigation of charge transport in nanostructured semiconducting materials such as graphene, nanowires, and nanocrystals and their device applications; and in the theory of charge, heat, and spin transport in nanomaterials.

Prof. Jena is a recipient of several awards including two best student paper awards in 2000 and 2002 for his Ph.D. dissertation research, the National Science Foundation (NSF) CAREER award in 2007, the Joyce Award for excellence in undergraduate teaching in 2010, the ISCS Young Scientist, and an IBM Faculty Award in 2012.

Huili Grace Xing (Member, IEEE) received the B.S. degree in physics from Peking University, Beijing, China, in 1996, the M.S. degree in material science from Lehigh University, Bethlehem, PA, USA, in 1998, and the Ph.D. degree in electrical engineering from the University of California Santa Barbara, Santa Barbara, CA, USA, in 2003.



She is currently the John Cardinal O'Hara CSC Associate Professor of Electrical Engineering at the University of Notre Dame, Notre Dame, IN, USA. Her research focuses on development of III-V nitride and 2-D crystal semiconductor growth, electronic, and optoelectronic devices based on compound and 2-D semiconductors, especially the interplay between material properties and device developments. More recent research interests include tunnel field-effect transistors and terahertz applications. She has authored/coauthored 120+ journal papers, 50+ conference publications, and 200+ conference presentations including over 40 invited talks.

Prof. Xing is a recipient of a U.S. Air Force Office of Scientific Research (AFOSR) Young Investigator Award and the National Science Foundation (NSF) CAREER Award.